

Department of Physics and Astronomy
University of Heidelberg

Bachelor Thesis in Physics
submitted by

Robin Eberhard
born in Aalen, Germany

handed in on
March 28, 2016

Characterization of a multispecies imaging system

This Bachelor Thesis has been carried out by Robin Eberhard at the
Institute for Theoretical Physics in Heidelberg
under the supervision of
Prof. Dr. Matthias Weidemüller

Characterization of a multispecies imaging system

Robin Eberhard

Abstract Lorem ipsum dolor sit amet, consectetur adipiscing elit. Ut purus elit, vestibulum ut, placerat ac, adipiscing vitae, felis. Curabitur dictum gravida mauris. Nam arcu libero, nonummy eget, consectetur id, vulputate a, magna. Donec vehicula augue eu neque. Pellentesque habitant morbi tristique senectus et netus et malesuada fames ac turpis egestas. Mauris ut leo. Cras viverra metus rhoncus sem. Nulla et lectus vestibulum urna fringilla ultrices. Phasellus eu tellus sit amet tortor gravida placerat. Integer sapien est, iaculis in, pretium quis, viverra ac, nunc. Praesent eget sem vel leo ultrices bibendum. Aenean faucibus. Morbi dolor nulla, malesuada eu, pulvinar at, mollis ac, nulla. Curabitur auctor semper nulla. Donec varius orci eget risus. Duis nibh mi, congue eu, accumsan eleifend, sagittis quis, diam. Duis eget orci sit amet orci dignissim rutrum.

Zusammenfassung Lorem ipsum dolor sit amet, consectetur adipiscing elit. Ut purus elit, vestibulum ut, placerat ac, adipiscing vitae, felis. Curabitur dictum gravida mauris. Nam arcu libero, nonummy eget, consectetur id, vulputate a, magna. Donec vehicula augue eu neque. Pellentesque habitant morbi tristique senectus et netus et malesuada fames ac turpis egestas. Mauris ut leo. Cras viverra metus rhoncus sem. Nulla et lectus vestibulum urna fringilla ultrices. Phasellus eu tellus sit amet tortor gravida placerat. Integer sapien est, iaculis in, pretium quis, viverra ac, nunc. Praesent eget sem vel leo ultrices bibendum. Aenean faucibus. Morbi dolor nulla, malesuada eu, pulvinar at, mollis ac, nulla. Curabitur auctor semper nulla. Donec varius orci eget risus. Duis nibh mi, congue eu, accumsan eleifend, sagittis quis, diam. Duis eget orci sit amet orci dignissim rutrum.

Contents

1. Introduction	1
2. Setup for high resolution imaging	2
2.1. Experimental requirements	2
2.1.1. Experimental setup	2
2.1.2. Basics of CCD cameras	3
2.1.3. Atom imaging	4
2.2. Camera for double species imaging	4
2.2.1. Comparison with the present setup	4
2.2.2. Dark current	5
2.2.3. Readout noise	6
2.2.4. Quantum efficiency	7
2.2.5. Pixel correlations	7
2.3. Mechanical shutter	7
2.3.1. Electronic setup	7
2.3.2. Dynamical properties	8
2.4. Mask for the CCD sensor	9
2.4.1. Fast kinetics mode	9
2.4.2. Frequency response of a slit	10
2.4.3. Optimization of the masking setup	11
3. Testing the camera: Superfluids	12
4. Conclusion and outlook	13
A. Acquisition sequence	14
B. Testing software	15

1. Introduction

- Nothing yet...

2. Setup for high resolution imaging

2.1. Experimental requirements

2.1.1. Experimental setup

The atoms in our trap are confined in a vacuum chamber, which has windows in x,y and z direction for the incident lasers, to either trap or image the atoms in the center. The double species camera (Andor iKon M) is placed along the z axis, above the chamber on a breadboard, where it is also possible to switch to another camera.

A biconvex lens focuses the imaging beam onto the CCD camera. To minimize the incident background light, the imaging path is covered in SM3 tubes, which can be directly connected to the camera due to a custom made front panel (see Appendix image).

The camera is also very sensitive to stray light, so that it has to be protected between measurements with a shutter, that covers the front end of the imaging path, such that no light will enter the camera, which will be covered in more detail in Section 2.2.5

Appendix
image

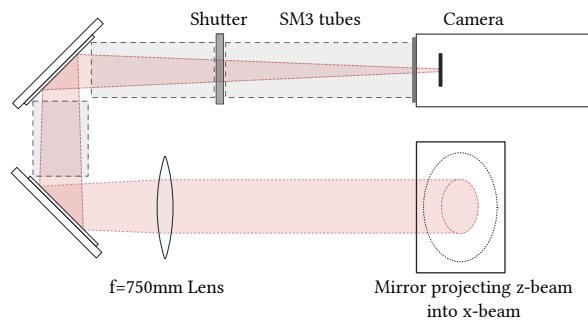


Figure 2.1.: **Imaging path.** The camera stands on a breadboard, together with the mirrors, the lens and the SM3 tube. The imaging beam originates from the z-axis (pointing out of the document), then transversing as shown.

2.1.2. Basics of CCD cameras

Cameras operate by means of converting photons first into electrons then into voltage and finally read out as data.

The photons are collected on an array of semiconductors, called the pixels, where ideally the spacing between the pixels is zero to get maximum accuracy. The resolution is then dependent on the pixel size, which is for scientific cameras usually between $10\text{ }\mu\text{m}$ and $20\text{ }\mu\text{m}$. Bigger pixels means higher photon sensitivity but usually lower resolution.

To create the digital image, the pixels have to be shifted into the analog digital converter (ADC). This is done, by vertically shifting them into the readout register and then horizontal into the ADC, where the charges are multiplied and converted to digital data.

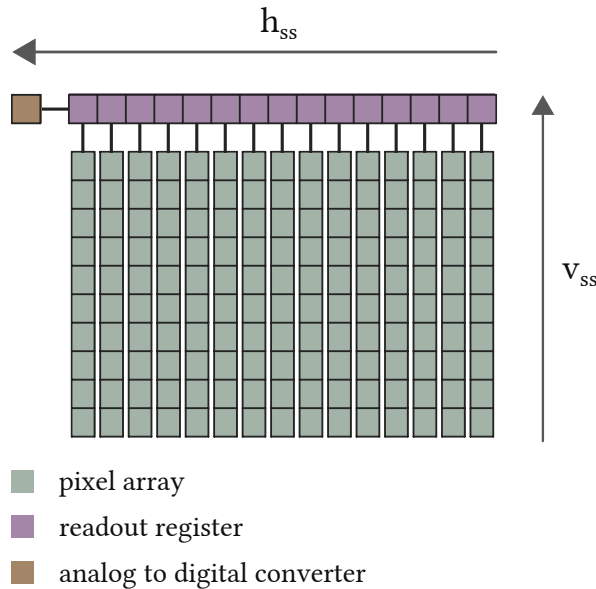


Figure 2.2.: **CCD scheme.** The pixels are arranged in the pixel array. During readout they are shifted upwards into the readout register and then to the side into the analog to digital converter

The shifting is done by storing the charges after collecting them. Each storage can be seen as an electronic potential. To successfully shift the charges and prevent overlapping, three potentials U_1 , U_2 and U_3 are necessary. Figure 2.3 indicates the systematics behind the shifting.

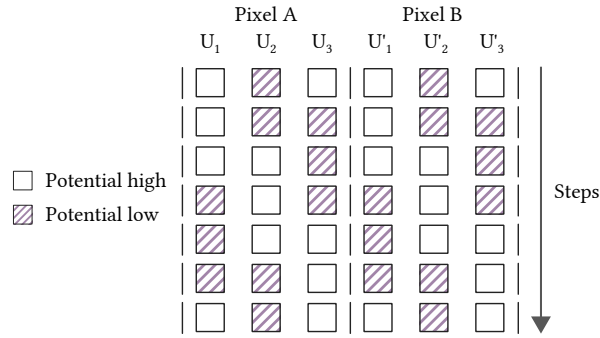


Figure 2.3.: **Shifting charges.** To shift charges from Pixel A to Pixel B, the potentials have to be set accordingly to allow the charge flow without overlapping each other. The drawing illustrates the charges moving from Pixel A to B, each row indicates the next step. Moving electrons to the next potential is a three-step process. The charges are first only present in the low potential U_i , while U_{i+1} is kept high, then distributed across U_i and U_{i+1} by setting them both low and at last U_i will be set high such that the charge is now fully in U_{i+1} .

2.1.3. Atom imaging

2.2. Camera for double species imaging

2.2.1. Comparison with the present setup

For the application of imaging small atom clouds, it is very important to have cameras with optimal noise reduction and maximal readout speed. The new setup improves on both attributes, with the ability to cool the chip down to reduce the dark noise as well as the fast kinetics mode, making it possible to acquire all images before reading out, improving the speed at which images can be taken significantly.

The old setup used a Guppy-38B camera, which is a lot smaller than the Andor iKon M ($48.2 \text{ mm} \times 30 \text{ mm} \times 30 \text{ mm}$ vs $204.2 \text{ mm} \times 105 \text{ mm} \times 107 \text{ mm}$), therefore making an implementation on a full experimental table easier. To implement such a complicated camera system that the Andor is, a lot of preparation was made in the thesis of Carmen.

better
title

not
sure
if it
makes
sense
to write
about
this
chapter

add ref-
erence
to Marc
Repp

reference
carmen

Nevertheless, despite its size, the new camera offers the ability to image both Lithium and Caesium species at once, while two Guppy cameras were needed beforehand, which also meant placing them on different imaging axes.

When comparing the resolution, the chip size also has to be considered. Since higher resolutions seem to be preferable at first, it also means that for the same pixel sizes, the photon sensitivities will decrease. The pixel sizes compare to $11\text{ }\mu\text{m}$ to $13\text{ }\mu\text{m}$ from the old versus the new setup respectively, while the resolutions are 768×492 and 1024×1024 making a larger magnification now possible.

As already mentioned, the readout speed is highly important in our setup. Since absorption imaging is the technique of choice to measure atom attributes, three images need to be taken each sequence, being the absorption, division and background image. For the Guppy camera, at a frame rate of 30fps, this meant the acquisition was finished after 100 ms. The Andor camera on the other hand can take images quickly without the need to read out inbetween. At the fastest shift speed, the acquisition is finished after 1.2 ms.

2.2.2. Dark current

- Theory on Dark current
- Temperature dependent
- Logarithmic dependency
- Water cooling

would be great to have maybe an image of the atoms with the old and new setup (maybe same cooling steps etc.)

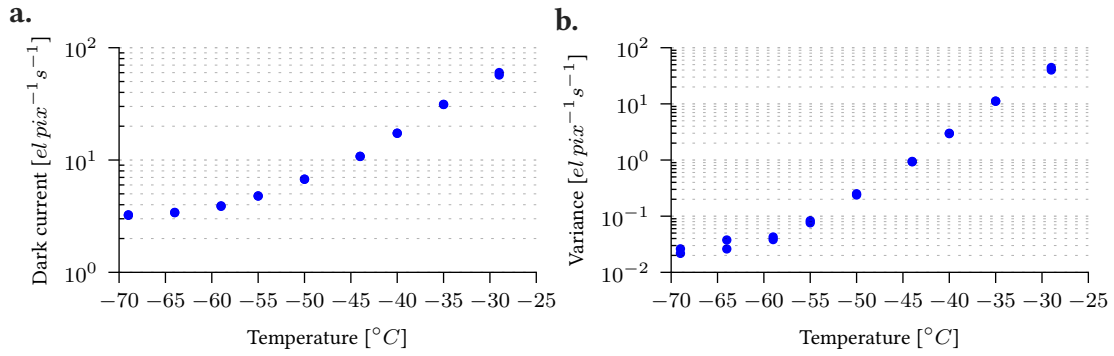


Figure 2.4.: **Dark noise.** The dark noise follows a power law dependency. Since these measurements were taken without water cooling installed, deviations are visible as the temperature reaches -70°C . The convergence to zero on the counts and their variance indicates accurate imaging when low temperatures are used. Gain in this measurement was minimal and the exposure time set to 100 s, such that dark current was the dominant noise source.

2.2.3. Readout noise

- How does pixel shifting work?

As seen in Chapter 2.1.2, pixels get shifted in order to be read out. Moving charges from pixel to pixel causes noise to accumulate over each iteration. In theory, this is visible as a gradient since each shift adds new charges due to excitations in the semiconductors. A possible characterization of this effect is to simply take the variance of an image.

Although the shifting gradient is not visible in the final picture, since it is removed by subtracting the background image, it is still important to minimize the noise originating from shifting the charges, which was found to be the case for minimal readout speed, see Figure 2.5.

This is intuitive, since shifting charges means increasing and decreasing potential wells, so that they can move from one into the other. If this is done fast enough, electrons are more likely to excite others from the valence to the conduction band, therefore adding noise.

Add
refer-
ence

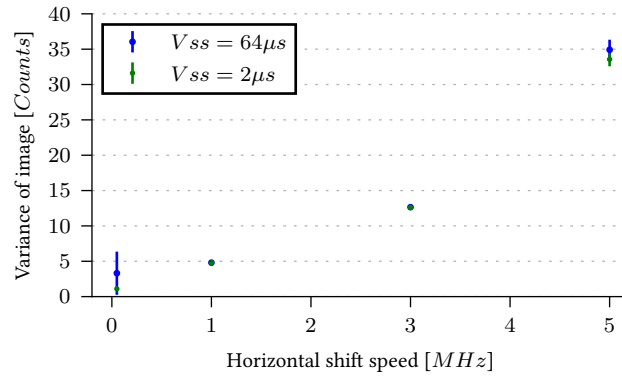


Figure 2.5.: **Readout noise.** The pixels are shifted row-wise into the readout register, depending on the vertical shift speed (v_{ss}) and then moved pixel-by-pixel with the horizontal shift speed into the analog to digital converter. Since noise reduction is important, minimal horizontal shift speeds will be used, while the vertical shift speed does not seem to affect the variance. To make the readout the dominant noise source, temperature was set to -69°C and exposure to 10 ms.

2.2.4. Quantum efficiency

- Little bit of theory
- Reference to Carmens' thesis

2.2.5. Pixel correlations

- Mainly the measurement (TBD)
- Some example images here maybe?

2.3. Mechanical shutter

2.3.1. Electronic setup

- A simplified circuit
- Explanation of the parts

2.3.2. Dynamical properties

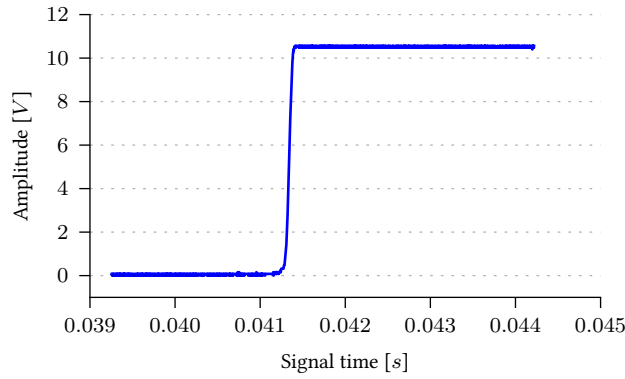


Figure 2.6.: **Shutter characterization.** The dynamics of the shutter were measured using a laser with a variable horizontal offset, which is fixed in this plot, and a photodiode measuring the laser intensity. For various offsets, error functions were fitted yielding the time until the shutter opens to this offset.

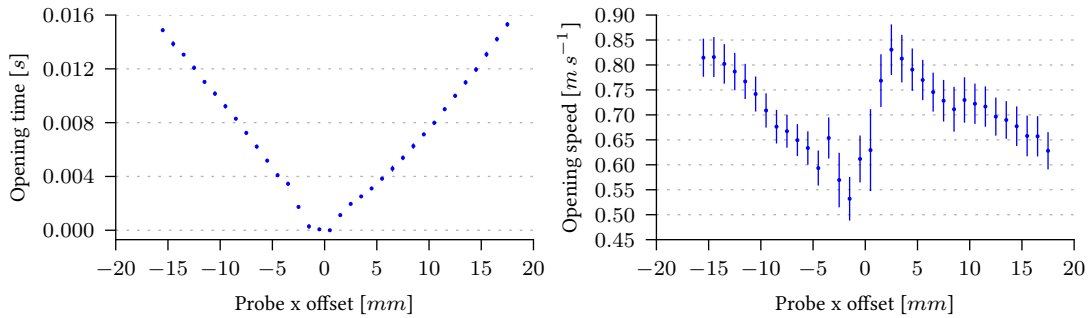


Figure 2.7.: **Sample dynamics.** Opening velocity was measured using the beam diameter and the time the shutter needed to transverse it. It is noticeable, that the opening velocity on the right side is faster at first than on the left side. This is due to the structure of the shutter, as can be seen in [Appendix image of shutter]. The overall opening speed on the other hand is not affected by this and seems to be linear with the offset.

appendix
image

2.4. Mask for the CCD sensor

2.4.1. Fast kinetics mode

- Why it is good
- Shifting timescales

2.4.2. Frequency response of a slit

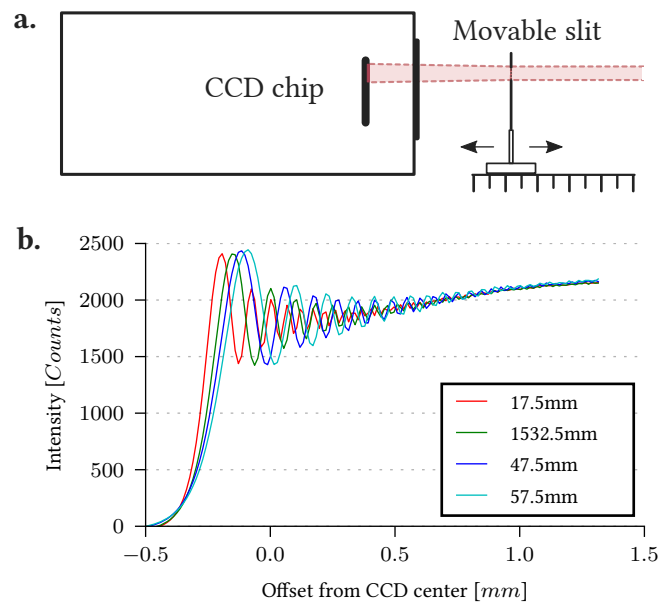


Figure 2.8.: **Distance dependant diffraction.** **a.** A slit was placed on a movable platform and diffraction was measured for various offsets. **b.** The diffraction frequency rises as the distance gets closer to the CCD. As soon as the frequency is of the order of one pixel, the diffraction is unnoticable, therefore higher frequencies, or closer slit positions are preferred.

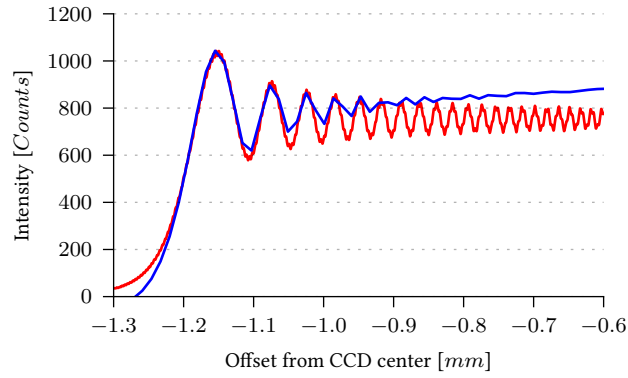


Figure 2.9.: **Diffraction measurement.** In order to characterize the diffraction on the CCD, a slit was placed as close as possible. The parameters were then measured as distance $d = 10.9$ mm, opening $a = 2.5$ mm using a ruler, and wavelength $\lambda = 852$ nm from the laser specifications. The blue curve is the experimental data, while the red curve was fitted, leaving distance and opening free. They were found to be $d' = (11.0 \pm 0.3)$ mm and $a' = (2.470 \pm 0.013)$ mm, which is in close agreement.

2.4.3. Optimization of the masking setup

- Custom slit properties

3. Testing the camera: Superfluids

- Theory on superfluids
- Spin population profile
- Measurement

4. Conclusion and outlook

A. Acquisition sequence

B. Testing software

List of Figures

2.1. Imaging path	2
2.2. CCD scheme	3
2.3. Shifting charges	4
2.4. Dark noise	6
2.5. Readout noise	7
2.6. Shutter characterization	8
2.7. Sample dynamics	8
2.8. Distance dependant diffraction	10
2.9. Diffraction measurement	11